Breakdown of disordered media by surface loads

Jakob Knudsen
Materials Science, Malmö University, SE 205 06 Malmö, Sweden and Solid Mechanics, Lund University, SE 221 00 Lund, Sweden

A. R. Massih
Materials Science, Malmö University, SE 205 06 Malmö, Sweden and Quantum Technologies, Uppsala Science Park, SE 751 83 Uppsala, Sweden

(Received 18 October 2004; revised manuscript received 13 June 2005; published 29 September 2005)

We model an interface layer connecting two parts of a solid body by N parallel elastic springs connecting two rigid blocks. We load the system by a shear force acting on the top side. The springs have equal stiffness but are ruptured randomly when the load reaches a critical value. For the considered system, we calculate the shear modulus G as a function of the order parameter ϕ describing the state of damage, and also the "spalled" material (burst) size distribution. In particular, we evaluate the relation between the damage parameter and the applied force and explore the behavior in the vicinity of material breakdown. Using this simple model for material breakdown, we show that damage, caused by applied shear forces, is analogous to a first-order phase transition. The scaling behavior of G with ϕ is explored analytically and numerically, close to $\phi=0$ and $\phi=1$ and in the vicinity of ϕ_c, when the shear load is close to but below the threshold force that causes material breakdown. Our model calculation represents a first approximation of a system subject to wear induced loads.

DOI: 10.1103/PhysRevE.72.036129 PACS number(s): 05.65.+b, 62.20.Mk, 64.60.Fr

I. INTRODUCTION

The damage of solids subject to external loads is a progressive physical process, which eventually may lead to material breakdown. At the microscopic scale, damage is caused by the localization of the stress field in the neighborhood of defects or at interfaces that induce the breaking of the atomic bonds. At a mesoscopic scale there is the interaction and coalescence of microscopic cracks or vacancies (voids), which together initiate a macroscopic crack.

One category of material damage problems, of great technological and fundamental interest, is the deterioration of solid surfaces in contact induced by relative motion. These problems belong to the field of tribology, in which friction and wear of materials are studied [1,2]. The first phenomenological approach to the problem of wear dates back to the 1940s, when Holm [3] provided a simple description for wear of solids, which later was rederived and applied by Archard [4]. The Holm-Archard wear description states that the amount of wear or the worn mass between two rubbing surfaces is proportional to sliding work (or dissipation energy due to friction) divided by the hardness of the surface; simply $m \propto F_N x/p$, where m is the worn mass, F_N the normal force or the force applied normal to the interface, x the distance slid, and p the penetration hardness, which is related to the surface tension of the solid, γ, in the manner $p \propto \gamma^3$ (see [2]). A mass loss from a solid body associates with heat dissipated to the environment, or from thermodynamics, $dQ \leqslant T\,dS$, where dQ is the increment of heat exchange, T the temperature, and dS the change in entropy. A shear force F_S applied to one of the bodies in a direction parallel to the interface plane, causes slip (a relative motion between parts of the interface) when $F_S=\mu F_N$, where μ is the coefficient of friction. This is Amontons' second law of macroscopic friction, formulated more than 200 years ago [1]. Setting $dQ=\mu F_N dx$ and $\mu=G/p$, with G denoting the shear strength of the softer material, we can express the Holm-Archard description as $dm \leqslant T\,dS/G$, i.e., the worn mass is proportional to the production of entropy and inversely to the shear strength of the softer material.

The aim of our study is to investigate the manner in which a solid material breaks down, when it is subjected to a shear force that reaches a certain critical value, by using a simple model for material damage. The system under study is described by N parallel elastic springs connecting two rigid blocks. The system is loaded with a shear force acting on the top side. If the relative motion is slow and the system is well cooled, it is possible to neglect the heat generated at the contact. Furthermore, neglecting the influence of the normal load, which mainly introduces compressive stresses, and supposing that the crack path is limited to the interface between the solid blocks, we arrive at the system studied in this paper. The model can represent rupture of a weld between two solid bodies due to shear forces.

A solid body subject to stress can be considered as being in a metastable state. It can transform in a self-organized manner to a stable fracture state by formation of cracks. This self-organized behavior of debonding in solids, which is the start of the damage process, is theoretically analogous to the phenomenon of nucleation in first-order phase transition [5–7]. Zapperi *et al.* [8,9] have utilized this analogy to study the global breakdown of disordered media under external loads. They used a two-dimensional lattice model, in which each bond of the lattice represents an elastic spring that breaks when it is stretched beyond a threshold value governed by a probability distribution. They studied numerically the random fuse model (RFM) and a spring network in the framework of a mean-field theory. They observed that the breakdown is preceded by avalanche events, which is analogous to the formation of the droplets observed near a spinodal decomposition [10,11].

The lattice or discrete modeling approach to material damage dates back to the 1926 work of Peirce, which is presently known as the global sharing fiber bundle [12]. Peirce considered N parallel fibers, each with its own rupture threshold. The fibers were linked in such a way that when one link failed, the load was transformed to and shared equally among all the intact links. Later, Daniels [13] studied and extended this model in detail and determined the asymptotic distribution of the bundle strength for large N. Sornette [14] evaluated the failure characteristic of N independent vertical lines linked in parallel with identical spring constants and random failure thresholds. He showed that the rupture properties of this system are quite distinct from systems that are linked in series. Furthermore, Sornette identified different regimes of rupture depending on the range of stresses: (i) an elastic-reversible behavior for stresses below a certain threshold σ_1 at which the first link failed, (ii) a stress range $\sigma_1 \leqslant \sigma_N$, where the system exhibited a nonlinear elastic but reversible behavior, and finally, (iii) for $\sigma \geqslant \sigma_N$ global failure. Moreover, Sornette showed that the asymptotic properties of global failure threshold of the network system can be explained in terms of the central limit theorem of statistics. A review of rupture models can be found in Sornette's book [15]. The book by Hermann and Roux offers a review of the field up to 1990 [16]. Hemmer and Hansen [17] studied and calculated the distribution of burst avalanches in fiber bundles. They found that for a large class of failure threshold distributions, the bursts are distributed according to an asymptotic scaling law $s^{-5/2}$ for simultaneous rupture of s fibers.

In this paper, we pursue a similar approach as Zapperi *et al.* [9] to investigate analytically and numerically the breakdown of disordered media subject to surface loads. We envisage that the solid, subjected to shear loading, contains an interface layer, which consists of a network of parallel springs. We study the behavior of the shear modulus, the order parameter characterizing the state of damage and burst (avalanche) size distribution. We compare the universality of our results with some other failure models, e.g., the fiber bundle models, and discuss our results in the context of the magnetic system.

The organization of this paper is as follows. In Sec. II, we present the physical model and its associating constitutive relations. In Sec. III, we outline the method of computation, numerical and analytical, for the evaluation of the shear modulus, the variation of the applied load with the order parameter, the critical exponents, and the avalanche size distribution. The results of our computations are presented in Sec. IV and discussed in Sec. V.

II. MODEL

Consider an interface layer connecting two parts of a solid body consisting of N equi-spaced parallel springs of equal length l with spring constants k_j and *randomly distributed* rupture deformation thresholds D_j, where $j \in [1,N]$. Initially the spring constants will be set equal ($k_j=k$). If a spring is stretched beyond its rupture threshold, it will lose its load carrying capacity, i.e., $k_j=0$. The springs are loaded with a force F acting parallel to the upper surface simulating the shear component of a wear-inducing load (Fig. 1). Each spring carries the load $F_j=k_j\Delta_j$, where $\Delta_j=l_j-l$ denotes the displacement of spring j. Assuming linear deformation, the deformation of spring i can be written as

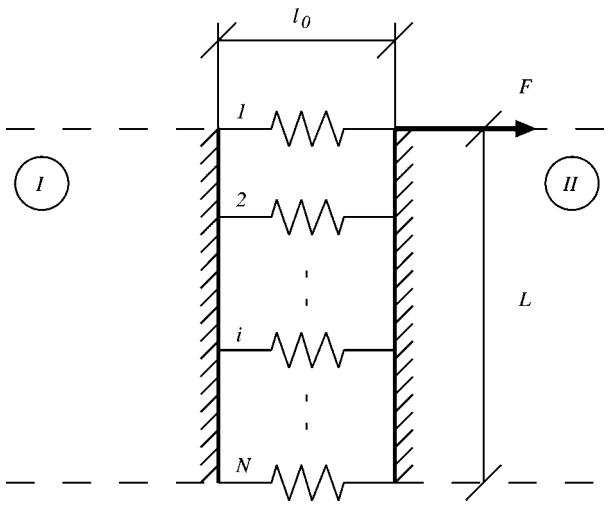

FIG. 1. N parallel springs, connecting bodies I and II, subjected to a shear load F.

$$\Delta_i = \frac{N-i}{N-1}\Delta_1 + \frac{i-1}{N-1}\Delta_N, \tag{1}$$

where Δ_1 and Δ_N are the displacements of the end springs. The state of equilibrium gives

$$F = \sum_{i=1}^{N} F_i = \sum_{i=1}^{N} k_i\Delta_i, \quad \sum_{i=2}^{N} F_i(i-1)a = 0, \tag{2}$$

where the equation on the right states that the sum of the moments of all the forces acting on the body is zero and a denotes the lattice spacing. Equations (1) and (2) are combined to find the boundary displacements

$$\Delta_1 = F(N-1)\left(\sum_{i=1}^{N} k_i(N-i) - \frac{\sum_{i=2}^{N} k_i(i-1)(N-i)}{\sum_{i=2}^{N} k_i(i-1)^2} \times \sum_{i=1}^{N} k_i(i-1) \right)^{-1}, \tag{3}$$

$$\Delta_N = -\Delta_1 \frac{\sum_{i=2}^{N} k_i(i-1)(N-i)}{\sum_{i=2}^{N} k_i(i-1)^2}. \tag{4}$$

Let us introduce the dimensionless variables $\kappa_i=k_i/k$, $\varepsilon_i=\Delta_i/l$, $r_i=D_i/l$, and $f=F/(klN)$; then Eq. (1) gives the expression for the strain of spring i, *viz.,*

$$\varepsilon_i = NfK_i \equiv Nf\left(\frac{X_i^N}{\sum_{j=1}^{N}\kappa_j X_j^N}\right), \tag{5}$$

where

$$X_i^N = (N-i) - S_N(i-1), \quad S_N \equiv \frac{\sum_{i=2}^{N}\kappa_i(i-1)(N-i)}{\sum_{i=2}^{N}\kappa_i(i-1)^2}, \tag{6}$$

with properties $X_N^N=-S_N X_1^N$ and $\kappa_i=\Theta(1-\varepsilon_i/r_i)$, where $\Theta(x)=1$ for $x>0$ and $\Theta(x)=0$ for $x<0$.

We now express the total dissipated energy due to breaking of springs,

$$E = \frac{1}{2}\sum_{i=1}^{N} k_i(\Delta_i^2 - D_i^2), \tag{7}$$

which can be rewritten in terms of the dimensionless variables in the form

$$\mathcal{E}\{\kappa\} \equiv \frac{E}{kl^2} = \frac{1}{2}\sum_{i=1}^{N}\kappa_i(\varepsilon_i^2 - r_i^2). \tag{8}$$

We further rewrite this equation in terms of the external applied force f using Eq. (5), *viz.,*

$$\mathcal{E}\{\kappa\} = \frac{1}{2}\left(\frac{Nf^2}{G\{\kappa\}} - \sum_{i=1}^{N}\kappa_i r_i^2\right), \tag{9}$$

where $G\{\kappa\}$ is given by

$$G\{\kappa\} = \left(N\sum_{j=1}^{N}\kappa_j K_j^2\right)^{-1}. \tag{10}$$

Here, G can be interpreted as a global shear modulus of the lattice. It depends on the number of broken springs and the order in which the springs break.

We define the order parameter for the system

$$\phi = \frac{1}{N}\sum_{i}^{N}\kappa_i. \tag{11}$$

Then Eq. (9) is expressed in the form

$$\mathcal{E} = \frac{1}{2}\sum_{i=1}^{N}\kappa_i\left(\frac{f^2}{\phi G(\phi)} - r_i^2\right), \tag{12}$$

where $G(\phi)$ is reexpressed as a function of the order parameter. As has been shown by Zapperi *et al.* [9], in analogy with the random field Ising model [18], the self-consistency requirement on ϕ yields the following integral equation (see, e.g., the Appendix in [19]):

$$\phi = 1 - \int_0^{f/\sqrt{\phi G(\phi)}} \psi(r)dr, \tag{13}$$

where $\psi(r)$ is the probability distribution function for the system breakdown.

The susceptibility χ for the system breakdown is then calculated according to

$$\chi \equiv \frac{d\phi}{df} = -\frac{y\psi(y)}{f - y^2\psi(y)h_\phi}, \tag{14}$$

where

$$y = \frac{f}{\sqrt{\phi G(\phi)}}, \quad h_\phi = \frac{1}{2}\frac{G(\phi)+\phi G'(\phi)}{\sqrt{\phi G(\phi)}}, \tag{15}$$

with $G'=dG/d\phi$. At the onset of breakdown, $f=f_c$ and $\phi=\phi_c$, the susceptibility diverges; this corresponds to

$$y_c\psi(y_c) = \frac{2\phi_c G(\phi_c)}{G(\phi_c)+\phi_c G'(\phi_c)}, \tag{16}$$

with $y_c=f_c/[\phi_c G(\phi_c)]^{1/2}$. We note that by specifying the form of the distribution function ψ, Eq. (16) determines $G(\phi_c)$. In particular, for $\psi=c$, where c is a constant, the differential equation (16) can be solved to give

$$G(\phi_c) = \frac{c^2 f_c^2}{\phi_c(\phi_0 - \phi_c)^2}, \tag{17}$$

where $\phi_0>\phi_c$ is an integration constant, which can be determined by computation.

For $f<f_c$, in the vicinity of f_c, the susceptibility scales as [9]

$$\chi = \frac{d\phi}{df} \sim (f_c - f)^{-1/2}. \tag{18}$$

Similarly, the corresponding description for the order parameter is

$$\phi - \phi_c \sim (f_c - f)^{1/2}. \tag{19}$$

Both relations (18) and (19) are the mean-field theory predictions (see, e.g., the Appendix in [19]).

The shear modulus $G(\phi)$ is expected to obey, in general, a universal scaling law for $\phi\approx 0$, in the form

$$G(\phi) = G_0\Theta\left(\phi - \frac{1}{N}\right)\phi^\tau, \tag{20}$$

where G_0 is a material constant and τ is a universal constant determined by experiment or computation. It is determined by rearranging Eq. (20),

$$\tau = \lim_{\phi\to 0}\frac{\ln|G(\phi)|}{\ln|\phi|}. \tag{21}$$

Finally in our analysis, we consider the concept of burst avalanche distribution [17]. This concept has relevance to a system undergoing wear, for which the size of the avalanches can be used to estimate the size of the wear fragments. The size of a burst avalanche, s, in our system is defined as the number of springs that break simultaneously for a constant

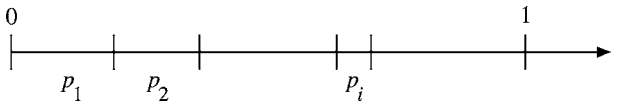

FIG. 2. Illustration of how the sequence of breaking of springs is determined from a random number generated according to a uniform distribution [see Eq. (23)].

load [20]. The burst size distribution $\mathcal{N}(s)$, is generated by counting the number of bursts of size s that occur as the system breaks down. Hemmer and Hansen [17] showed that for a large class of failure threshold distributions in the fiber bundle models, the bursts are distributed according to an asymptotic power law,

$$\lim_{N\to\infty} \frac{\mathcal{N}(s)}{N} \sim s^{-\xi}, \tag{22}$$

with a universal exponent $\xi=5/2$.

III. COMPUTATION METHOD

The mean-field theory presented above requires as input the shear modulus G. Once the state of the system is known, i.e., the number and position of the ruptured links is known, the shear modulus of the system can be determined from Eq. (10). However, the position of the ruptured springs depends on the sequence in which they rupture. The sequence, in turn, depends on the local rupture thresholds and the applied force. Even for moderate system sizes ($N\sim 1000$) the number of possible sequences to failure becomes prohibitively large; hence a statistical method is needed to generate an average, or "most probable," shear modulus curve as a function of the order parameter ϕ. We take two different approaches to accomplish this: (a) a numerical scheme and (b) an analytic procedure. We compare the mean-field predictions with quasistatic simulations of the lattice breakdown.

A. Numerical scheme

The probability that the spring i breaks first under a uniform strain field is $p=1/N$, since the rupture limits are selected from the same distribution. Here the springs are subjected to a linear strain field, meaning that the probability that the spring i breaks first can be written in the form

$$p_i = w_i p \quad \text{with } w_i = \frac{\epsilon_i^+}{\sum_{i=1}^{N} \epsilon_i^+}, \tag{23}$$

where w_i is a weighting factor based on the local strains ϵ_i^+ of the springs and the plus superscript indicates that only positive strains are counted [cf. Eq. (5)].

The sequence of spring ruptures is then determined numerically by selecting a random number from a uniform distribution in the interval [0,1], and breaking the corresponding spring (see Fig. 2). The rupture probabilities, according to Eq. (23), are then recomputed and a new rupturing spring is selected. The procedure is repeated until a complete path to total failure is established. The average shear modulus curve is then found by averaging over several such sequences. Finally, simple regression analysis is made to find a suitable polynomial or power law expression approximating the average shear modulus curve.

A *quasistatic* method is used to perform the numerical simulations of the breakdown of the spring system (Fig. 1). The simulation is initiated by associating a rupture limit to each individual spring in the system. The limits are chosen from a predefined distribution. A full set of rupture limits is called a configuration. For each configuration, the computation starts with all links intact, $\kappa_i=1$, and the external load equal to zero, $f=0$. Next, the load is incremented and the local strains are computed according to Eq. (5). The local strains are then compared to their respective rupture limits. If the local strain exceeds the rupture limit, then the link is broken, i.e., the local stiffness is set equal to zero. If a rupture has occurred, the local strains are recomputed and checked once more against the rupture thresholds, otherwise the computation proceeds with the next load increment. When only one spring remains, the load loop is interrupted and the computation proceeds to the next configuration.

Three different failure distribution functions are studied here: (i) a uniform distribution in the interval $r_i \in [0;2]$,

$$\psi(r) = \begin{cases} \frac{1}{2}, & r \in [0,2], \\ 0, & \text{otherwise;} \end{cases} \tag{24}$$

(ii) a Weibull distribution with shape factor $\nu=2$ and location parameter $\lambda=1$,

$$\psi(r) = \begin{cases} \dfrac{\nu}{\lambda}\left(\dfrac{r}{\lambda}\right)^{\nu-1} e^{(r/\lambda)^{\nu}}, & r \geqslant 0, \\ 0, & r < 0; \end{cases} \tag{25}$$

(iii) a Gaussian (normal) distribution with mean value $\vartheta=1$ and standard deviation $\sigma=1$,

$$\psi(r) = \frac{1}{\sigma\sqrt{2\pi}} e^{-(r-\vartheta)^2/2\sigma^2}. \tag{26}$$

The critical values ϕ_c and f_c can be estimated directly from the mean-field analysis from Eq. (16). For the uniform distribution this equation is easily solved, leading to a functional relationship between f_c and ϕ_c. For the Weibull and normal distributions, a Newton-Raphson scheme is employed to find the load corresponding to a given value of the order parameter, by finding the roots of Eq. (16). The result is a line in the (ϕ_c, f_c) plane, which can be compared with the critical values from the quasistatic simulations.

B. Analytical procedure

The material constant G_0 [cf. Eq. (20)] is determined exactly when all the springs are intact, i.e., at $\phi=1$. For this case, Eq. (10) reduces to the following simple relation:

$$G_{\phi=1} = G_0 = \frac{1+N}{-2+4N}. \tag{27}$$

Hence, as $N\to\infty$, $G_0\to 1/4$. The exact expression for G consists of terms like $\Sigma_{i=1}^{N}\kappa_i$, $\Sigma_{i=1}^{N}\kappa_i i$, and $\Sigma_{i=1}^{N}\kappa_i i^2$. With only

one spring broken, denoted by j, the sums can be evaluated:

$$\sum_{i=1}^{N} \kappa_i = N - 1, \tag{28}$$

$$\sum_{i=1}^{N} \kappa_i i = N^2/2 + N/2 - j, \tag{29}$$

$$\sum_{i=1}^{N} \kappa_i i^2 = N^3/3 + N^2/2 + N/6 - j^2. \tag{30}$$

Hence, the slope of G for $\phi \approx 1$ can be determined, once the position of the first spring rupture is known, *viz.,*

$$\left.\frac{dG}{d\phi}\right|_{\phi=1} \approx \frac{G(1) - G(1 - 1/N)}{1/N}. \tag{31}$$

We note that the first spring breaks according to a linear distribution [cf. Eq. (23)], which is identified by $j = \text{int}[2(N-1)/9]$ where int$[a]$ converts a value to integer type. It corresponds to the average value of the linear distribution. Inserting this j into Eqs. (29) and (30), then evaluating Eq. (31) and letting $N \to \infty$, leads to $(dG/d\phi)|_{\phi=1} = \frac{4}{9}$. Consequently, the following linear approximation of G is found:

$$G_{\phi \approx 1} = \frac{4}{9}\phi - \frac{7}{36}. \tag{32}$$

For the system under study, the Nth spring is always the last to break, since it is subject to compressive load. Moreover, the shear modulus is zero when only one spring remains intact. When only two intact springs remain in the system, denoting the next to last spring to break as m, the sums in G [cf. Eqs. (28)–(30)] are evaluated:

$$\sum_{i=1}^{N} \kappa_i = 2, \tag{33}$$

$$\sum_{i=1}^{N} \kappa_i i = N + m, \tag{34}$$

$$\sum_{i=1}^{N} \kappa_i i^2 = N^2 + m^2. \tag{35}$$

Inserting Eqs. (33)–(35) in Eq. (10) and using $\phi = 2/N$, it is possible to carry out the limit analysis in Eq. (21), once the position of penultimate spring rupture is identified.

The springs closest to the lower side of the system (cf. Fig. 1) are subject to compressive stresses during the major part of the breakdown process. Assuming that the compressive stresses are sufficiently large, it is possible to identify the next to last rupture as $m = N - 1$. Carrying out the limit analysis leads to $\tau = 3$. Hence, the analytic approximation for G in the limit $\phi \approx 0$ becomes

$$G_{\phi \approx 0} = \frac{1}{4}\phi^3 \sim |\phi|^3. \tag{36}$$

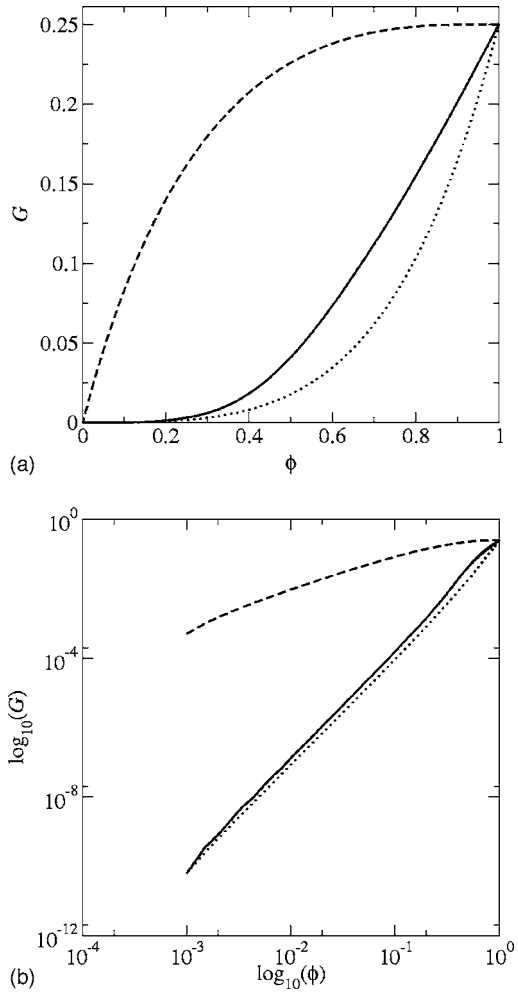

FIG. 3. Numerical simulation of $G(\phi)$ averaged over 100 randomly ordered series of ruptures of 2001 springs, solid line. The dotted and dashed lines depict the lower and upper bounds of G, respectively. (a) and (b) show linear and logarithmic plots, respectively.

IV. RESULTS

The results of our computations of the shear modulus, the order parameter vs the applied shear force, and the burst size distribution are displayed in a number of figures. Figures 3(a) and 3(b) show the shear modulus averaged over 100 rupture sequences of 2001 springs. The sequences were generated according to the procedure described in Sec. III A. This curve, henceforth, is called the average shear modulus curve. These figures also show the lower and and upper bounds of $G(\phi)$, respectively. The lower bound curve corresponds to the breaking of the highest strained spring and the upper curve to the breaking of the least strained spring. From these figures, it can be deduced that $G(\phi)$ depends linearly on ϕ close to $\phi = 1$, while it has a scaling behavior (power law dependence) close to $\phi = 0$ [cf. Eq. (20)]. Note that the average and lower bound shear modulus curves coalesce as $\phi \to 0$ [see Fig. 3(b)]. This validates the assumption that spring $N-1$ is the second last to break and consequently Eq. (36) is correct.

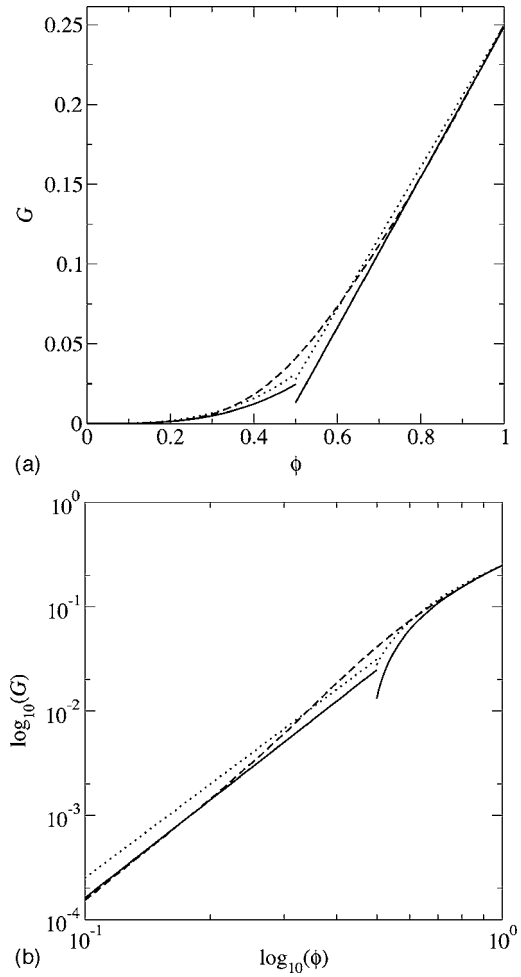

FIG. 4. Approximate computations of the shear modulus $G(\phi)$. The solid and dotted lines display numerical and analytical approximations, respectively. The broken line shows the curve found from averaging over several sequences of spring ruptures (see Fig. 3).

Using regression, linear and power law expressions are fitted to the computed data. Here, the intervals $\phi \in [0^+;0.25]$ and $\phi \in [0.75;1.0]$ are chosen to determine the power law and linear law, respectively. Our analysis leads to the following expressions for $G(\phi)$:

$$G_{\phi \approx 0} \sim 0.217 \phi^{3.1297}, \tag{37}$$

$$G_{\phi \approx 1} \sim -0.222\,59 + 0.471\,54\phi. \tag{38}$$

Figures 4(a) and 4(b) show the analytical [Eqs. (32) and (36)] and numerical [Eqs. (37) and (38)] scaling and linear laws, respectively, superimposed on the average shear modulus curve. As can be expected, the approximated curves deviate for ϕ in the mid-range ($\phi \sim 0.5$).

A system size of $N=10\,001$ springs and a load increment of $\Delta f = 0.01/N$ are used in the numerical simulations (the quasistatic method discussed in the foregoing section) presented here. To gather enough data for statistical predictions, each simulation is repeated for $M=1000$ different configurations of rupture thresholds r. Values from the last load step before global breakdown are taken as critical values. Figure 5(a) displays the simulated critical values of the order parameter ϕ_c and the shear force f_c, for the uniform, Weibull, and normal distribution functions defined in Eqs. (24)–(26). The three distributions display similar results with respect to scatter in f_c and ϕ_c [see Figs. 5(b) and 5(c)]. Using these results [average values of $G(\phi_c), \phi_c$, and f_c], we have determined ϕ_0 in Eq. (17) for the uniform failure distribution given by Eq. (24). We found $\phi_0 = 1.042$.

Next, we focus on the relationship between the scaling variables ϕ and f. Figures 6(a)–6(c) show the computed order parameter ϕ plotted against the applied load f for the three distributions using the quasistatic method. The data presented in the figures are averaged over 1000 configurations of rupture thresholds. The displayed (ϕ, f) plane is divided into rectangles. The arithmetic mean of the values confined within each rectangle is used to represent the data in the figures. The number of points within each rectangle is utilized as the weighting factor to fit a scaling law expression Eq. (19) to the simulated data. The scaling form of the order parameter predicted by the mean-field theory, Eq. (19), is also depicted in Figs. 6(a)–6(c). The simulated data support the validity of the mean-field analysis.

Finally, the important concept of burst distribution is explored. For a system undergoing wear, the size of the avalanches can be used to estimate the size of the wear fragments [2]. The size of an avalanche or burst, s, is defined as the number of springs that break simultaneously for a constant load [20]. The burst size distribution is generated by counting the number of bursts of size $N(s)$ occurring as the system breaks down. Figures 7(a)–7(c) show the burst distributions for the three chosen rupture threshold distributions for the damage model considered here. The three figures display similar behavior. The figures also include a line with a slope $-5/2$ (log-log scales), which is the theoretical result found for a fiber bundle model with global load sharing [17,21]. The results indicate that this scaling law has relevance for the system studied here.

V. DISCUSSION

The results presented in the preceding section show that the average shear modulus is linearly proportional to the damage in the beginning of the breakdown process and has power law characteristics at end of the process (see Fig. 3). Consequently, the shear modulus can be approximated with simple relations, which do not require knowledge of the path to failure, i.e., the order in which the springs break. The critical force and critical order parameter (damage) can be estimated analytically using mean-field theory once the shear modulus has been determined, provided that the distribution of the disorder of the material is known. Here, it is assumed that the disorder is quenched in the system and does not change during the breakdown process [16].

In the preceding sections, we showed that for $\phi \approx 0$, the shear modulus G scales as $G \sim \phi^{\tau}$, with $\tau = 3$, which we obtained by analytical calculation, while numerical simulations led to $\tau \approx 3.13$ in the interval $\phi \in [0^+;0.25]$. These results may be compared with properties of other condensed matter systems, e.g., the macroscopic conductance in a resistor net-

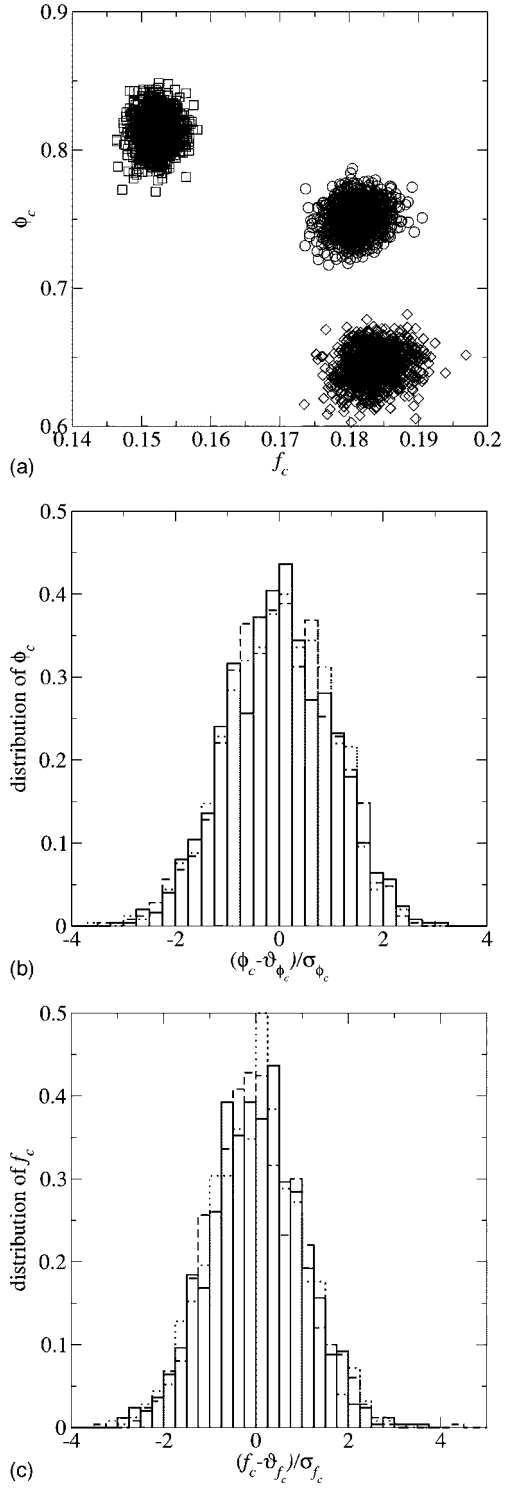

FIG. 5. (a) The critical scaling variables ϕ_c versus f_c for 1000 configurations, computed by the quasistatic method, of uniformly $r_i \in [0;2]$, Eq. (24), circles; Weibull $(\nu,\lambda)=(2,1)$, Eq. (25), squares; and normal $(\vartheta,\sigma)=(1,1)$, Eq. (26), diamonds, distributed rupture thresholds of $N=10\,001$ springs. (b) and (c) display normalized histogram distributions of ϕ_c and f_c, respectively. Solid, dotted, and dashed lines refer to the uniform, Weibull, and normal distribution, respectively. The abscissas have been rescaled with the mean value ϑ and the standard deviation σ to enable comparison between results for the three rupture threshold distributions.

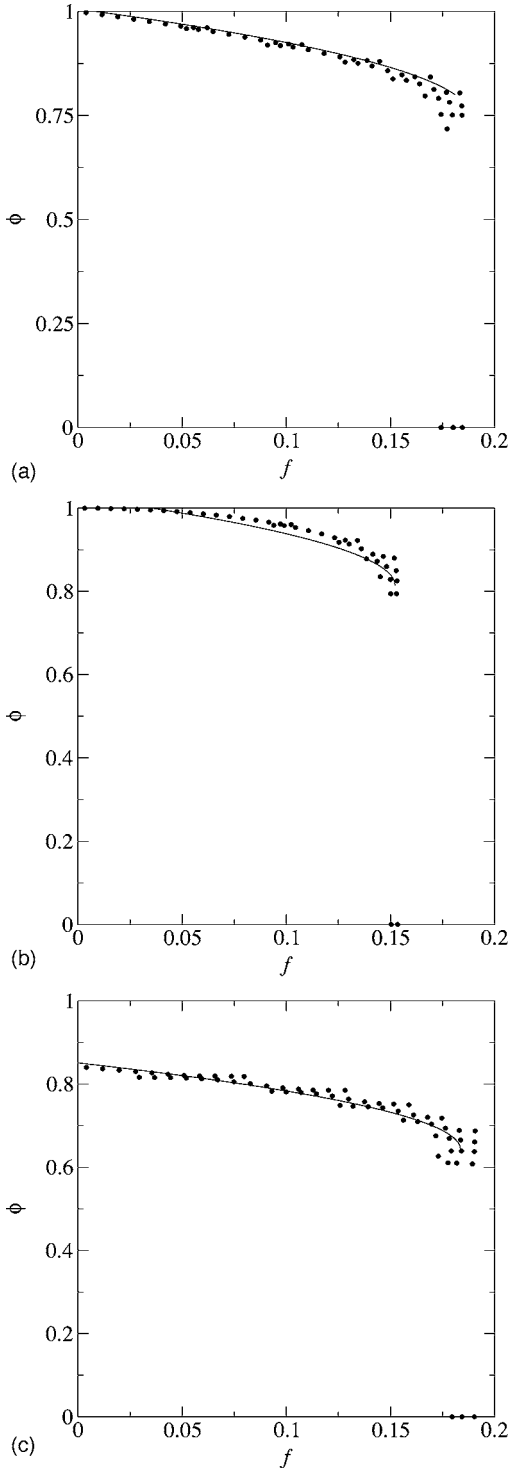

FIG. 6. The damage order parameter ϕ versus the shear force f averaged over 1000 configurations, computed by the quasistatic method of (a) uniform $r_i \in [0;2]$, (b) Weibull $(\nu,\lambda)=(2,1)$, and (c) normal $(\vartheta,\sigma)=(1,1)$ distributions of rupture thresholds for $N=10\,001$ springs, respectively. The lines represent the mean-field scaling behavior.

work or the elastic modulus of gels in a polymer system [22]. For lattice dimensions $d \geqslant 6$, which corresponds to a mean-field approximation, de Gennes found that $\tau=3$. This result also conforms with a recent calculation by Xing *et al.* of the

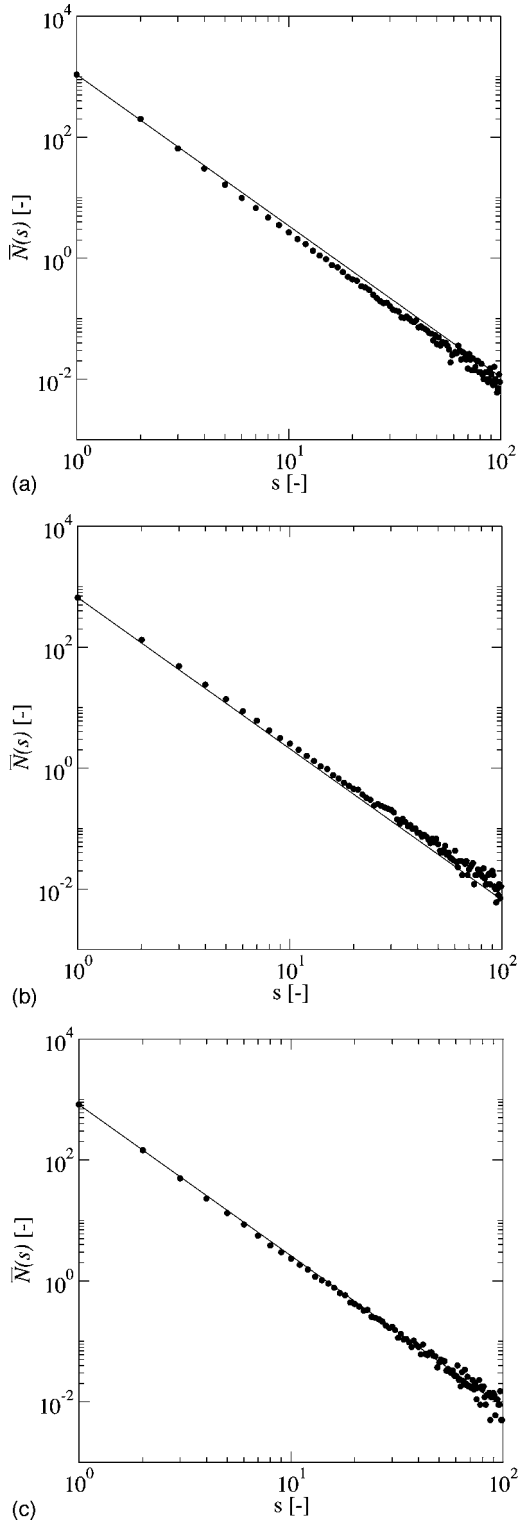

FIG. 7. Burst size distributions averaged over 1000 configurations using (a) uniform $r_i \in [0;2]$, (b) Weibull $(\nu,\lambda)=(2,1)$, and (c) normal $(\vartheta,\sigma)=(1,1)$ probability distributions of rupture thresholds for $N=10\,001$ springs. The straight lines have a slope of -2.5 [see Eq. (22)].

scaling behavior of the shear modulus in a polymer system [23]. Their renormalization group analysis shows that $\tau=3-\frac{5}{21}\epsilon$, with $\epsilon=6-d$, which is identical to the conductivity exponent of the random resistor network calculated by Harris and Lubensky [24].

The constitutive relation for damage, ϕ vs f, for all three statistical distributions [Figs. 6(a)–6(c)] indicates that ϕ decreases slowly with the increase in f; then a sharp (discontinuous) drop in ϕ occurs, when the shear force reaches a threshold value f_c. This sudden transition in the order parameter and the fact that the scaling form given by Eq. (19) describes the approach to f_c so well $(f<f_c)$ indicates that material breakdown is a first-order phase transition, e.g., similar to a spinodal decomposition [10].

The burst distributions for the system using the three statistical distributions are displayed in Figs. 7(a)–7(c). Here the size distribution of avalanches is integrated over the load. For a fiber bundle model (FBM) with global load sharing (the load is evenly distributed over the remaining fibers) the expected number of avalanches $\mathcal{N}(s)$, where s is the size of the avalanche, scales as $\mathcal{N}\sim s^{-\xi}$, with $\xi=5/2$ [17,21]. Although this scaling law holds for a large class of threshold distributions, this is not always the case [25]. A regression analysis, using the numerical data shown in the figures, gives an exponent close to the FBM value, 2.5 ± 0.1.

It may be worth comparing our results with the random-field Ising model predictions, which intend to describe the behavior of many magnetic materials subjected to external magnetic field H. For this system, the magnetization changes through nucleation and motion of domain walls. The motion is discrete, i.e., there will be magnetization bursts corresponding to reorganization (or avalanche) of a domain of spins which span several decades of size [26]. There will be plenty of small avalanches of spins and fewer and fewer avalanches of larger and larger sizes [27]. The power law dependence for the probability of having an avalanche of a given size has been determined [26]. It is shown that the size distribution of all avalanches that occur in one branch of hysteresis loop (for H from $-\infty$ to $+\infty$) scales in the form $\mathcal{N}_{int}\sim s^{-\theta}\mathcal{F}(s,r)$, where $\mathcal{N}_{int}$ is the integral of $\mathcal{N}$ over the external field, $\mathcal{F}$ is a scaling function, and r is a "disorder" parameter [28]. The mean-field computation of Perković *et al.* [28] at a give value of r near the critical point resulted in $\theta=\frac{9}{4}$, which is close to the corresponding value predicted by the FBM. However, near the low-ordered disordered phase close to the spinodal line the mean-field avalanche exponent is calculated to be $\theta=\frac{5}{2}$ (see Appendix A.5 of Dahmen and Sethna [29]).

The breakdown of the system that we considered is similar to that of the FBM. The process of breakdown is envisaged to proceed by the formation of microcracks. The microcracks are nucleated according to a linear distribution function, which is proportional to the displacement field. The cracks grow to a critical size and coalesce to form the final crack. We found no indication that a single crack takes over and dominates the breakdown process. This behavior was also found in a two-dimensional mesh subject to a uniform stress field [9].

VI. CONCLUSION

We modeled an interface layer by N parallel elastic springs that connected two rigid blocks. We loaded the sys-

tem by a shear force f acting on the top side. The springs were assumed to have equal stiffness but were ruptured randomly when the load reached a critical value f_c. The state of the material damage for the system was characterized by an order parameter ϕ varying between zero (complete breakdown) and 1 (intact). The shear modulus for the system was numerically simulated over the entire range of ϕ and it was found that $G_{\phi\approx 0} \sim \phi^{3.13}$ and $G_{\phi\approx 1} \sim \phi$. The linear behavior of $G(\phi)$ close to $\phi=1$ was confirmed analytically. Moreover, our analytical calculation showed that $G_{\phi\approx 0} \sim \phi^3$. We calculated ϕ vs f numerically and determined their values at the onset of breakdown, i.e., around (ϕ_c, f_c), and also found their variation depending on the failure distribution function selected. We noted that there was a discontinuous drop in ϕ around $f=f_c$. The mean-field theory predicted this behaviour for $f \lessapprox f_c$, leading to the conclusion that breakdown behaves like a first-order phase transition. Finally, we calculated the burst size distribution during rupture and found that the system behaves according to the predictions of the fiber bundle model.

The model presented here can be extended to treat a more realistic representation of wear induced loads by considering a two-dimensional lattice comprising a network of blocks connected to each other and to a rigid indenter by elastic springs.

ACKNOWLEDGMENT

The work was supported by the Swedish Foundation for Knowledge and Competence Development (KKS) under Award No. HG 212/01.

[1] F. P. Bowden and D. Tabor, *The Friction and Lubrication of Solids*, 2nd ed. (Oxford University Press, Oxford, 2001), Chap V.
[2] E. Rabinowicz, *Friction and Wear of Materials*, 2nd ed. (John Wiley & Sons, New York, 1995).
[3] R. Holm, *Electric Contacts* (Almquist & Wiksells, Stockholm, 1946).
[4] J. Archard, J. Appl. Phys. **24**, 981 (1953).
[5] Robin L. Blumberg Selinger, Z.-G. Wang, W. M. Gelbert, and A. Ben-Shaul, Phys. Rev. A **43**, 4396 (1991).
[6] A. Buchel and J. P. Sethna, Phys. Rev. Lett. **77**, 1520 (1996).
[7] A. Buchel and J. P. Sethna, Phys. Rev. E **55**, 7669 (1997).
[8] S. Zapperi, P. Ray, H. E. Stanley, and A. Vespignani, Phys. Rev. Lett. **78**, 1408 (1997).
[9] S. Zapperi, P. Ray, H. E. Stanley, and A. Vespignani, Phys. Rev. E **59**, 5049 (1999).
[10] W. Klein and C. Unger, Phys. Rev. B **28**, 445 (1983).
[11] C. Unger and W. Klein, Phys. Rev. B **31**, 6127 (1985).
[12] F. T. Peirce, J. Text. Inst. **17**, 355 (1926).
[13] H. E. Daniels, Proc. R. Soc. London, Ser. A **183**, 405 (1945).
[14] D. Sornette, J. Phys. A **22**, 243 (1989).
[15] D. Sornette, *Critical Phenomena in Natural Sciences: Chaos, Fractals, Selforganization and Disorder: Concepts and Tools* (Springer-Verlag, Berlin, 2000).
[16] *Statistical Models for the Fracture of Disordered Media*, edited by H. J. Hermann and S. Roux (Elsevier Science North-Holland, Amsterdam, 1990).
[17] P. C. Hemmer and A. Hansen, J. Appl. Mech. **59**, 909 (1992).
[18] J. P. Sethna, K. Dahmen, S. Kartha, J. A. Krumhansl, B. W. Roberts, and J. D. Shore, Phys. Rev. Lett. **70**, 3347 (1993).
[19] J. Knudsen and A. R. Massih, e-print cond-mat/040102280.
[20] G. C. Batrouni, A. Hansen, and J. Schmittbuhl, e-print cond-mat/0106558.
[21] A. Hansen and P. C. Hemmer, Phys. Lett. A **184**, 394 (1994).
[22] P. G. de Gennes, J. Phys. (France) Lett. **37**, 1 (1976).
[23] X. Xing, S. Mukhopadhyay, and P. M. Goldbart, Phys. Rev. Lett. **93**, 225701 (2004).
[24] A. B. Harris and T. C. Lubensky, Phys. Rev. B **35**, 6964 (1987).
[25] M. Kloster, A. Hansen, and P. C. Hemmer, Phys. Rev. E **56**, 2615 (1997).
[26] O. Perković, K. Dahmen, and J. P. Sethna, Phys. Rev. Lett. **75**, 4528 (1995).
[27] J. P. Sethna, K. A. Dahmen, and O. Perković, e-print cond-mat/0406320.
[28] O. Perković, K. Dahmen, and J. P. Sethna, Phys. Rev. B **59**, 6106 (1999).
[29] K. Dahmen and J. P. Sethna, Phys. Rev. B **53**, 14872 (1996).